ARMY RESEARCH LABORATORY

Macroscale and Microscale Structural Characterization of Cephalopod Chromatophores

by Keith M. Kirkwood, Eric D. Wetzel, George Bell, Alan M. Kuzirian, and Roger T. Hanlon

ARL-RP-0318 **April 2011**

A reprint from the *Proceedings of the Army Science Conference*, Orlando, FL, 29 November 2010.

NOTICES

Disclaimers

The findings in this report are not to be construed as an official Department of the Army position unless so designated by other authorized documents.

Citation of manufacturer's or trade names does not constitute an official endorsement or approval of the use thereof.

Destroy this report when it is no longer needed. Do not return it to the originator.

Army Research Laboratory
Aberdeen Proving Ground, MD 21005

ARL-RP-0318 **April 2011**

Macroscale and Microscale Structural Characterization of Cephalopod Chromatophores

Keith M. Kirkwood and Eric D. Wetzel
Weapons and Materials Research Directorate, ARL

and

George Bell, Alan M. Kuzirian, and Roger T. Hanlon
Marine Biological Laboratory
Woods Hole, MA 02543

A reprint from the *Proceedings of the Army Science Conference*, Orlando, FL, 29 November 2010.

REPORT DOCUMENTATION PAGE

Form Approved
OMB No. 0704-0188

1. REPORT DATE *(DD-MM-YYYY)*	2. REPORT TYPE	3. DATES COVERED (From - To)
April 2011	Reprint	

4. TITLE AND SUBTITLE
Macroscale and Microscale Structural Characterization of Cephalopod Chromatophores

5a. CONTRACT NUMBER
ORISE Contract 120-1120-99 (GHIORSE)

5b. GRANT NUMBER

5c. PROGRAM ELEMENT NUMBER

6. AUTHOR(S)
Keith M. Kirkwood, Eric D. Wetzel, George Bell, Alan M. Kuzirian, and Roger T. Hanlon

5d. PROJECT NUMBER

5e. TASK NUMBER

5f. WORK UNIT NUMBER

7. PERFORMING ORGANIZATION NAME(S) AND ADDRESS(ES)
U.S. Army Research Laboratory
ATTN: RDRL-WMM-A
Aberdeen Proving Ground, MD 21005

8. PERFORMING ORGANIZATION REPORT NUMBER
ARL-RP-0318

9. SPONSORING/MONITORING AGENCY NAME(S) AND ADDRESS(ES)

10. SPONSOR/MONITOR'S ACRONYM(S)

11. SPONSOR/MONITOR'S REPORT NUMBER(S)

12. DISTRIBUTION/AVAILABILITY STATEMENT
Approved for public release; distribution unlimited.

13. SUPPLEMENTARY NOTES
A reprint from the *Proceedings of the Army Science Conference*, Orlando, FL, 29 November 2010.

14. ABSTRACT
Cephalopods, the class of mollusks that include squid, cuttlefish, and octopus, possess skin with dynamic adaptable appearance. Their unique ability to rapidly change their visual appearance is enabled in part by a layer of skin containing thousands of chromatophore organs. These organs consist of a pigment sac connected to 15-25 radially arranged muscles. Muscle contraction and relaxation controls the expansion state of the sac, which alters the size of its presented area and the skin color. This study examines the chromatophore organs in detail, to investigate the global and local structure and characterize mechanical properties of skin from the squid *Loligo pealeii*. A biaxial membrane inflation test and digital image correlation was used to measure the biaxial modulus, strain limits, plus strain and damage fields on the skin during bulge experiments. Microscopy was used to examine chromatophore substructures and determine their connectivity and functional relationships with surrounding structures.

15. SUBJECT TERMS
Cephalopod, chromatophore

16. SECURITY CLASSIFICATION OF:			17. LIMITATION OF ABSTRACT	18. NUMBER OF PAGES	19a. NAME OF RESPONSIBLE PERSON
a. REPORT	b. ABSTRACT	c. THIS PAGE			Keith Kirkwood
Unclassified	Unclassified	Unclassified	UU	14	19b. TELEPHONE NUMBER (*Include area code*) (410) 306-1589

MACROSCALE AND MICROSCALE STRUCTURAL CHARACTERIZATION OF CEPHALOPOD CHROMATOPHORES

Keith M. Kirkwood*, Eric D. Wetzel
U.S. Army Research Laboratory, Weapons and Materials Research Directorate
Aberdeen Proving Ground, MD 21005

George Bell, Alan M. Kuzirian, and Roger T. Hanlon
Marine Biological Laboratory
Woods Hole, MA 02543

ABSTRACT

Cephalopods, the class of mollusks that include squid, cuttlefish, and octopus, possess skin with dynamic adaptable appearance. Their unique ability to rapidly change their visual appearance is enabled in part by a layer of skin containing thousands of chromatophore organs. These organs consist of a pigment sac connected to 15-25 radially arranged muscles. Muscle contraction and relaxation controls the expansion state of the sac, which alters the size of its presented area and the skin color. This study examines the chromatophore organs in detail, to investigate the global and local structure and characterize mechanical properties of skin from the squid *Loligo pealeii*. A biaxial membrane inflation test and digital image correlation was used to measure the biaxial modulus, strain limits, plus strain and damage fields on the skin during bulge experiments. Microscopy was used to examine chromatophore substructures and determine their connectivity and functional relationships with surrounding structures.

1. INTRODUCTION

Camouflage is utilized throughout nature, with some animals having the additional ability to change their appearance dynamically. One well known example of adaptive camouflage is exhibited by some species of chameleon, which are capable of predator specific changes of color and pattern (Stuart-Fox, *et al.*, 2008). The animals with the most dynamic and detailed adaptive camouflage are cephalopods – specifically, the Molluscan Class Cephalopoda including cuttlefish, octopus, and squid (Hanlon, 2007; Hanlon and Messenger, 1996; Hanlon, 1982; Hanlon and Messenger, 1988). These creatures can quickly change color, pattern, iridescence and texture (with the exception of the squid) to camouflage themselves against a wide range of backgrounds (Hanlon, *et al.*, 1990) (Figure 1a). Their unique dynamic camouflaging ability is enabled by a sequence of thin layers in its soft and stretchable skin (Mathger and Hanlon, 2007; Cloney and Florey, 1968) (Figure 1b). Beneath the transparent epidermis layer is a layer of thousands of pigmented chromatophores that are yellow, red, or brown. The next layer below contains structural reflectors called iridophores that reflect many spectra, ranging from near-IR to short-wavelength blues and greens (Hanlon and Messenger, 1996; Mathger and Hanlon, 2007). The combination of chromatophore pigments and structural reflectors allows the cephalopod to display dynamic patterning in complex combinations of color, iridescence, brightness, and polarity. The design of the chromatophore organs and the dermal layer are the focus of this investigation.

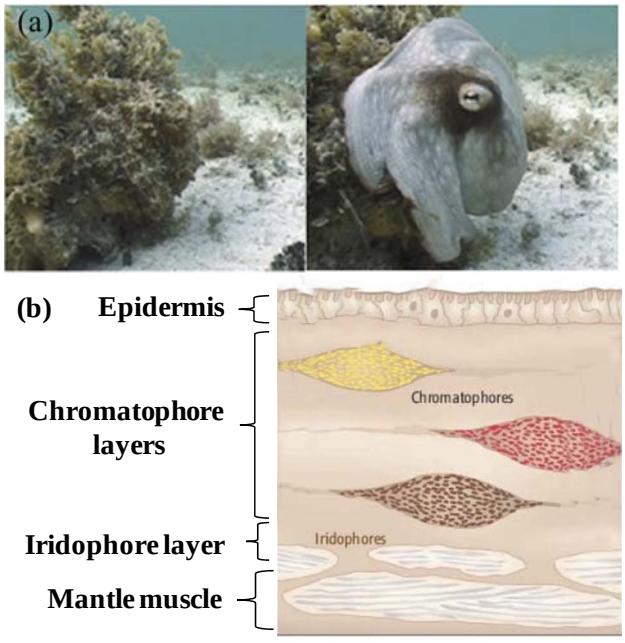

Figure 1: (a) *Octopus vulgaris* in transition from a concealed to an un-concealed state (Hanlon, 2007). (b) Schematic of squid skin structure (Hanlon and Messenger, 1996).

The chromatophore organ (Figure 2) contains a cytoelastic sac (*sacculus*) of pigment granules surrounded by a spoked array of 15 to 25 radial muscles (Cloney and Florey, 1968). The chromatophore organs alter their appearance through control of the visual presented area of

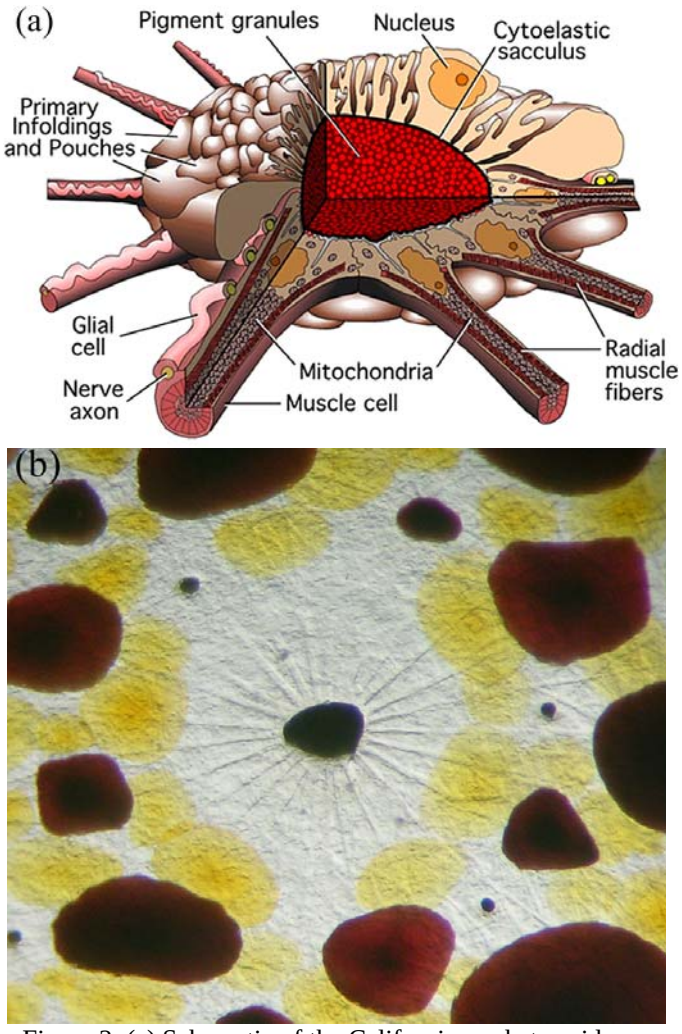

Figure 2: (a) Schematic of the California market squid, *Loligo opalescens*, chromatophore organ (Cloney and Florey, 1968). (b) Micrograph of live squid tissue (*Loligo pealeii*) illustrating radial muscle network attached to chromatophore pigment sac.

the pigment sac. Contraction of the radial muscles stretches the pigment sac from a punctate sphere into a flat disc of color, increasing the presented area (Messenger, 2001). Retraction of the sac back to the spherical shape after the muscles relax is believed to be driven by elastic recovery of the cytoelastic sacculus (Cloney and Brocco, 1968). The chromatophore size varies with species and color, yellow being the smallest and brown the largest. Typical chromatophore sizes are 10-100 μm in diameter when punctate and 0.1-1 mm when expanded (Hanlon 1982). A typical actuation of the chromatophore from "off" to "on" occurs in approximately 700 milliseconds for fast pattern execution.

Cephalopods are widely studied for their behavior (Hanlon and Messenger, 1996), eyesight (Sweeney, *et al.*, 2007), skin optical properties (Mathger and Hanlon, 2007), and neurological control of color change (Florey, 1969; Reed, 1995a; Reed, 1995b; Messenger, *et al.*, 1997; Cloney and Florey, 1968; Messenger, 2001). Studies of the structure of cephalopod skin have been primarily anatomical, leading to an understanding of the chromatophore ultrastructure (Cloney and Florey, 1968; Florey, 1969; Mirow, 1972) with detailed knowledge of muscle innervations (Reed, 1995a; Packard, 1995; Florey, 1966). However, a detailed analysis of the mechanical properties, structural connectivity, and dynamic interactions of the various dermal layers and substructures has not yet been reported.

In this paper, the structural properties of the squid chromatophore layer are reported from a combined engineering and biological perspective. The chromatophore layer was dissected from live squid and the bulk mechanical properties of the layer were characterized using a bulge inflation technique (Small and Nix, 1992). Inflation tests are commonly used for the biaxial testing of biological materials (Boyce, *et al.*, 2008; Sutton, *et al.*, 2008; Dick, 1951) to avoid potential complications with uniaxial test samples (Elsheikh and Anderson, 2005). In addition to bulk measurements, two-dimensional digital image correlation (DIC) was used to provide local strain field measurements of the tissue during the bulge test. DIC results are also reported for the skin surface above active chromatophores to probe the effect of actuation on the surrounding tissue. These measurements were used in conjunction with light microscopy techniques to look for physical coupling between chromatophores and to improve our understanding of the three-dimensional structure of the chromatophore organ.

2. EXPERIMENTAL

2.1 Squid Procurement

Squid (*Loligo pealeii*) were caught by otter trawls off of Cape Cod, MA and maintained in a large open seawater tank at the Marine Resources Center (Marine Biological Laboratory, Woods Hole, MA). Squid with minimal skin lacerations were chosen for tests to minimize disturbance of the tissue. The squid were decapitated and immediately dissected. Tissue samples will stay alive for hours after decapitation, and were stored at 4ºC between tests.

2.2 Bulge Test

To maintain tissue vitality, the tissue was submerged in room temperature seawater during dissection, sample mounting, and inflation testing. The squid tissue was prepared for bulge testing by first removing the epidermal layer, exposing the chromatophore dermal layer, while the tissue was still attached to the mantle. A rubber o-ring with inside diameter 20.4 mm (Buna N AS568A-019) was

then attached to chromatophore layer (Figure 3a) with cyanoacrylate glue (Loctite 411, Henkel). The squid was briefly removed from the seawater bath to adhere the moisture-cured glue that quickly bonded to the skin. By gluing the o-ring to the dermis while it was still attached to the mantle, the natural tension and dimensions of the *in-vivo* skin were maintained. The o-ring and skin were then removed from the mantle, and the iridophore layer, located sub-dermally relative to the chromatophore layer, was physically removed.

The inflation device consisted of a chamber with a 12.7 mm OD orifice. The chamber was submerged in salt water, and then the o-ring with chromatophore layer was clamped over the orifice with a small stainless steel shim (ID = 12.7 mm, OD = 19.05 mm, thickness = 0.41 mm). The chromatophore layer placed over the orifice separates the seawater within the chamber from the seawater of the surrounding bath. The surrounding bath remained at atmospheric pressure, while the chamber pressure could be manually via an attached syringe pump (Figure 3b). Chamber pressure was measured via a digital pressure gauge (MG1-5A-9V, SSI Technologies, Inc).

Experiments were conducted by driving the syringe pump until a target pressure was achieved. The side profile ("bulge") of the inflated skin was then photographed using a horizontally-mounted camera (Fuji I5 Pro with Nikon 18-105mm lens). Image analysis (ImageJ, NIH) was used later to analyze the photographs and extract quantitative bulge height values. Samples reported in this study were typically inflated multiple times, with increasing peak pressure during each cycle.

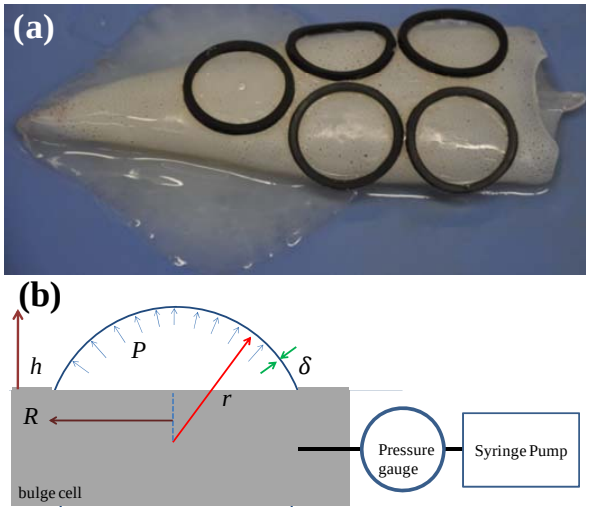

Figure 3: (a) Outer o-rings attached to chromatophore layer of squid during dissection. (b) Schematic of bulge test experiment with membrane analysis for inflation of spherical cap.

Because the ratio of the sample thickness (approximately ~0.5 mm from skin section micrograph measurements) to the principal radius of curvature was less than 0.1, the tissue could be treated as a thin membrane (Young and Budynas, 2002). The measured bulge height h at a given pressure P was used to calculate the stress and strain on the membrane (Figure 3b). The equibiaxial stress σ was calculated using the Young-Laplace law for inflation of spheres (Small and Nix, 1992; Xiang, *et al.*, 2005),

$$\sigma = \frac{P\left(R^2 + h^2\right)}{4h\delta}, \tag{1}$$

where R was the radius of the opening and δ was the membrane thickness. The biaxial strain was defined as the change in arclength divided by the original arclength (Small and Nix, 1992; Xiang, *et al.*, 2005)

$$\varepsilon = \frac{R^2 + h^2}{2Rh}\arcsin\left(\frac{2Rh}{R^2 + h^2}\right) - 1 \tag{2}$$

Equations 1 and 2 were combined to calculate the biaxial modulus, Y, according to.

$$Y = \frac{E}{1-\upsilon} = \frac{\sigma}{\varepsilon} \tag{3}$$

Equation 3 was fit to the stress-strain data to calculate the biaxial modulus.

2.3 Digital Image Correlation

Two-dimensional strain field measurements of live squid skin were performed using submerged, UV, micro-digital image correlation (DIC). A digital camera (Nikon D90) was attached to a long distance microscope lens (Model K2, Infinity Optical) focused on the peak of the bulge to image the surface deformation of the skin. A high-contrast pattern was placed on the skin (Figure 4) using 20-µm UV-sensitive pigment granules (UVXPBR, LDP, LLC). The powder was misted on to the skin by tapping a small diameter cotton swab above the skin. The images were taken with a UV flash to minimize exposure time (1/200 sec) and any effects of tissue motion on the DIC calculations. The UV flash consisted of a Nikon SB-600 AF Speedlight (Nikon USA) with the plastic diffuser replaced with a UV bandpass filter (B370, Edmund Optics). Videos of live chromatophores pulsing were taken with the Nikon D90 in movie mode with constant UV illumination from a high-powered lamp (Magnaflux ZB-100F).

The relative change in pattern appearance between images was analyzed with commercial software (VIC-2D, Correlated Solutions, Inc.) to provide quantitative, two-dimensional strain mappings for each image relative to a reference image. By using UV-fluorescing pigments to

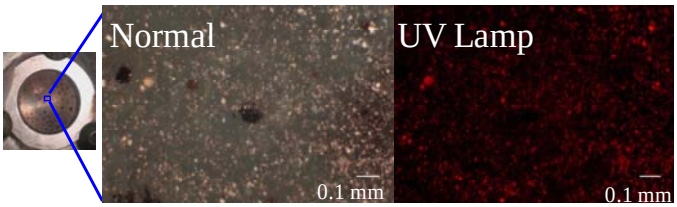

Figure 4: UV-sensitive pigment granules placed on skin to create high contrast pattern under UV illumination for DIC measurements.

generate the pattern, UV or white illumination could be used to selectively alternate between surface strain imaging and bulk optical imaging.

2.4 Microscopy

Specimens for microscopy were dissected in a similar manner to the bulge specimens. The skin was pinned out in a Sylgard® lined dissecting dish in fresh seawater to prevent desiccation. The epidermis was removed and the remaining dermal layer fixed using Holland's derivative of Bouin's fixative (Romeis, 1948). Samples were embedded in polyester wax (Steedman, 1947) and sectioned at 6μm thick. Skin sections were subsequently stained using Weigert's Iron Hematoxylin and counterstained with solution II of Mallory's triple connective stain, the Aniline Blue/Orange G solution (Mallory, 1944; Humason, 1967). Bright field images were collected using a Zeiss Axioscope (Carl Zeiss MicroImaging, Inc., USA) with total magnifications from 50X to 630X.

3. RESULTS

3.1 Bulge testing

Figure 5a illustrates the experimental results for the bulge test of a squid chromatophore layer. The peak pressure of each cycle was increased until the sample burst on cycle 7 (Figure 5b). The first two pressurization cycles of the test had similar peak pressures and demonstrated equivalent height-pressure and stress-strain behaviors (Figures 5a and 5c respectively). The first three inflation (I) curves were very similar, demonstrating repeatability of measurements. The maximum pressure of the third cycle exceeded the peak pressure of cycles 1 and 2 and changed the bulge response of the tissue. As the pressure was lowered on the 3rd deflation cycle (D), the behavior no longer followed that of the preceding inflation cycle, as it did for cycles 1 and 2. The height-pressure behavior of the 4th inflation cycle did not follow the low pressure behavior of the previous three cycles. This behavior suggested that some damage or structural change occurred to the tissue during cycle 3 inflation, after the pressure exceeded the maximum pressure of cycle 2, 1500 Pa. Figure 5c shows that the change occurred between a biaxial strain of 7 and 12%.

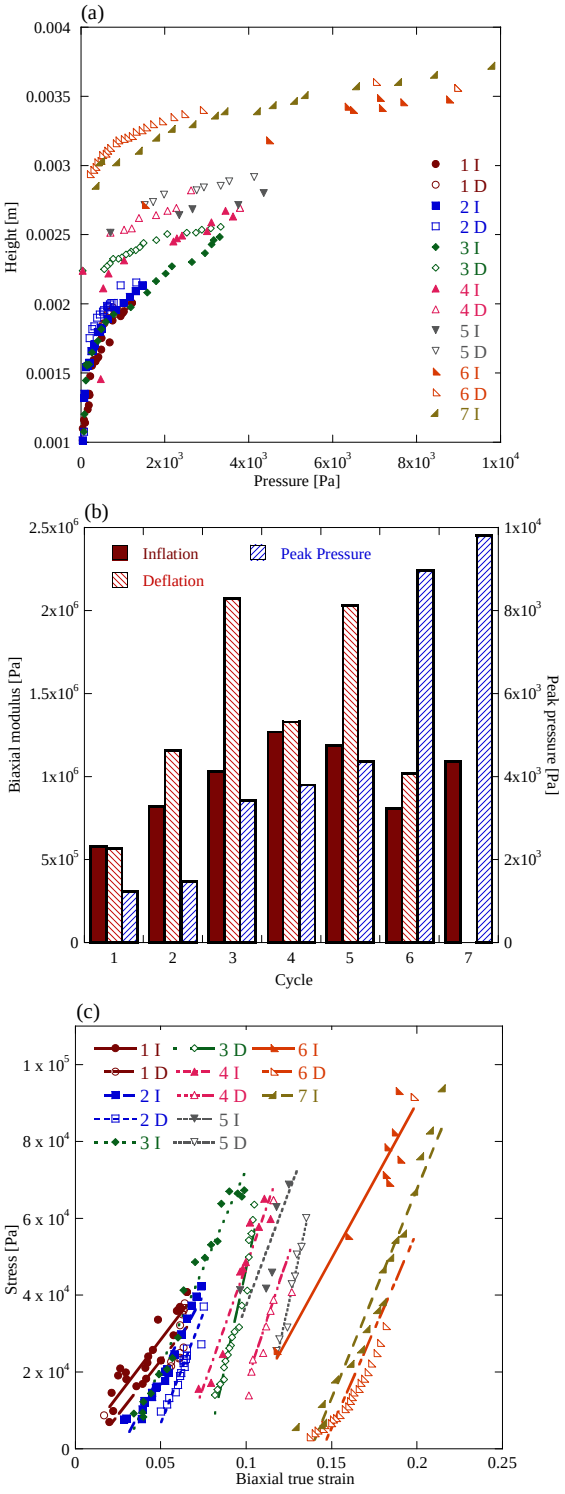

Figure 5: Experimental results for bulge test of squid chromatophore layer. Pressure cycles are labeled as either inflation (I) or deflation (D). (a) Bulge height versus applied pressure for each cycle. (b) Calculated biaxial modulus, Y, and maximum pressure for each pressure cycle (c) Stress-strain calculations for each pressure cycle fit with equation 3.

This strain value was close to the reported maximum strain value for collagen (Gosline, *et al.*, 2002), thus suggesting damage to the collagen within the connective tissue.

As the maximum pressure of each cycle increased, the low pressure qualitative behavior of the curves continued to change with the height no longer going to zero. In general, as the peak inflation pressure increased, the modulus calculated from the fit of the data increased (Figure 5b). Note that modulus value for the inflation stage of each cycle was always lower than the modulus value for the deflation stage of the cycle. The height-pressure curves developed a hysteresis as the deformation increased, which was associated with the change in collagen fiber configuration with strain (Fung, 1993). The repeatable behavior of cycles 1 and 2 suggested that preconditioning was not necessary for the sample.

The measured biaxial modulus increased by a factor of 2 between the first and seventh inflation cycles. The chromatophore layer burst at a strain of 21% but the mechanical behavior of the tissue appeared to be irreversibly changed at much smaller deformations.

Figure 6 displays the maximum principal strain field calculated with DIC from images taken during cycles 1, 2 and 4 from the experiment in Figure 5 (Table 1). The DIC calculated a strain field for the relative motion of the particles from the first image, shown in Figure 5a. When Figure 5a was taken, the bulk strain measured using the bulge technique was close to 0.02. Therefore, in order to compare the DIC strain values with those measured with the bulk technique (Table 1), the bulge strain values are reported as the difference between the calculated strain and the strain of the initial bulge height.

The patterning on the surface allows one to visualize damage to the tissue that might not otherwise be visible due to the sample transparency. Tears in the tissue show up as dark patches in the strain field. When the tissue tears, the natural tension of the tissue is released and sections of the tissue are pulled away from the tear. The underlying tissue, unseeded with particles, was exposed as a dark region in the images. Small tears in the tissue first became evident in Figure 6b and c. These images were taken at bulk strains between 2% and 12%, the values corresponding to damage to the tissue (Figure 5a).

In Table 1 the calculated strain from the bulge height and DIC measurements are compared. In general, the strains calculated from the motion of the particles on the surface with DIC are within 20% of the strain calculated from the bulge height with equation 2. Figure 6h demonstrates that the tears in the surface of the tissue (Figure 6) are not associated with obvious visible damage to the underlying chromatophore tissue or structures. In addition, the strain values were much higher local to the torn regions and show no distinguishable pattern that correlates with an underlying chromatophore (centered). These results suggest that the surface layer of tissue above the chromatophores themselves are decoupled mechanically, perhaps to protect the chromatophore from being damaged due to external trauma.

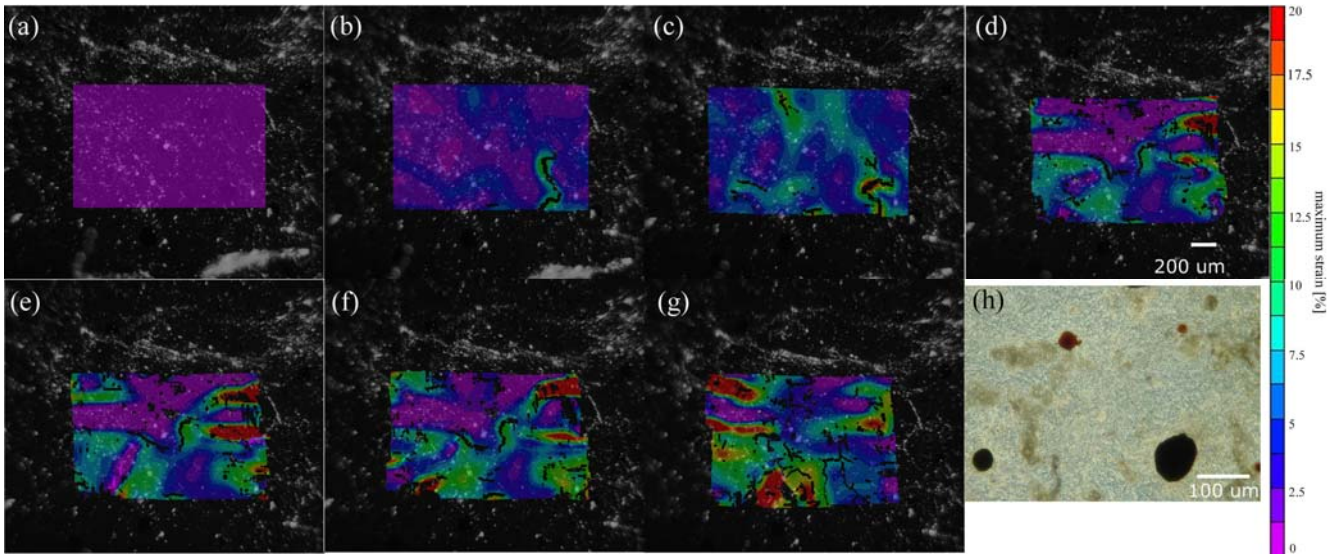

Figure 6:(a-g) DIC calculated maximum principal strain field from images taken during bulge test in Figure 5. Corresponding data for applied pressure and corresponding bulge height of each image are given in Table 1. (h) Visible light image of tissue at center of bulge

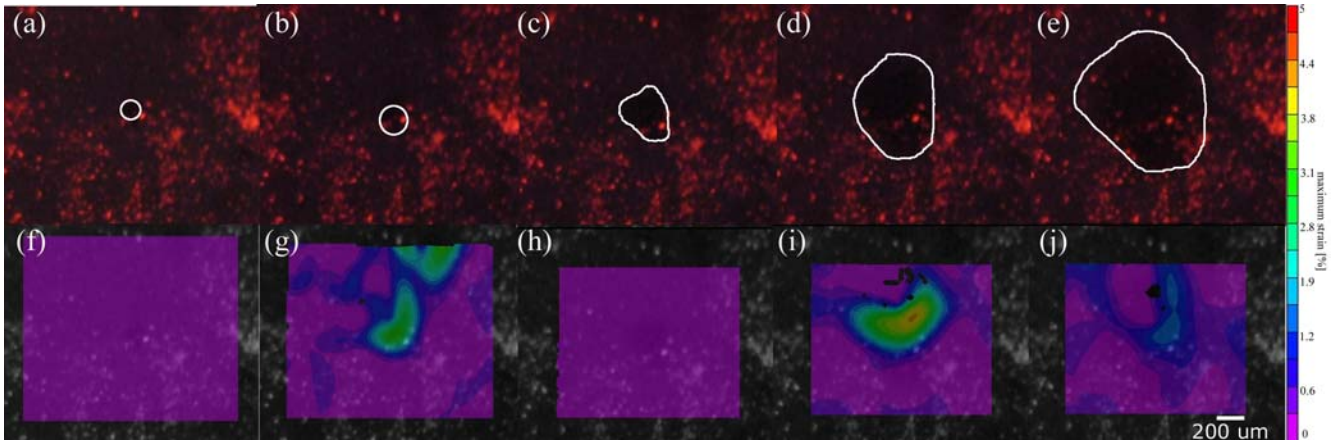

Figure 7: (a-e) Images of chromatophore layer with UV illuminated powder misted on surface of skin. White outline added around single chromatophore going from punctate (a) to expanded state (e). (f-j) DIC results for maximum principal strain field calculated for surface of skin in a-e.

3.2 DIC of actuating chromatophore

Figure 7 shows the strain field calculated with 2D-DIC for particles placed on the surface of the chromatophore layer above a pulsing chromatophore organ. A neuromodulator acetylcholine (ACh) was placed on the surface of the skin to induce active pulsing of the chromatophores (Messenger, 2001). Figure 7a-e are the UV illuminated images with an outline of the underlying brown chromatophore drawn in white. The change in presented area of the chromatophore was roughly 50:1. The calculated strain field for the pulsing sequence is given in Figure 7f-j. There was no measureable change in the strain field attributable to actuation of the chromatophore. The strain values were consistently low throughout chromatophore expansion. These results again reinforce the concept that the chromatophore actuation takes place without significant deformation of the dermal layers above the chromatophore.

3.3 Microscopy

Microscopy of dissected squid skin provides evidence that the chromatophores are isolated from the surrounding environment. Figure 8 displays a cross section of dissected squid tissue. Two colored chromatophores are visible in this image, a large expanded brown chromatophore (BC) and small contracted yellow chromatophore (YC). It was evident from these images that the chromatophores, in both expanded (flat) and contracted (circular) states, reside in a sinus surrounded by connective tissue. With chromatophore expansion, this void is filled with sheath cells (not visible in this section), that surround the cytoelastic sac (Cloney and Florey, 1968). The sinus encapsulating the chromatophore appeared to be the same size as the expanded chromatophore (BC in Figure 8). The size of the sinus does not appear to decrease as the chromatophore retracts (YC in Figure 8). It is possible that some distortion in the shape or cavity volume was due to sample preparation sectioning. However, these sectioned tissues demonstrate why the DIC of the skin surface did not reveal any motion.

Table 1: Strain calculations for bulge height data (Figure 5) and average strain values from DIC measurements (Figure 6).

Image	Cycle	Pressure [Pa]	Calculations from bulge			Biaxial strain difference*	maximum principal strain from image (DIC)
			Height [m]	Stress [Pa]	Biaxial strain		
a	1 I	4.14E+01	1.10E-03	6.95E+03	0.019	0.0000	0.000
b	1 I	6.83E+02	1.72E-03	3.36E+04	0.048	0.0283	0.027
c	2 D	1.32E+03	2.15E-03	3.71E+04	0.074	0.0550	0.053
d	4 I	5.31E+02	2.11E-03	1.57E+04	0.072	0.0521	0.045
e	4 I	7.45E+02	2.13E-03	2.15E+04	0.073	0.0536	0.055
f	4 I	1.03E+03	2.31E-03	2.47E+04	0.086	0.0661	0.060
g	4 I	3.79E+03	2.69E-03	6.47E+04	0.115	0.0958	0.081

*difference = $\varepsilon - \varepsilon_a$

The chromatophore also possesses radial muscles that originate on the cytoelastic sac, and attach to the inner walls of this sinus. With a section thickness of 6 µm radial muscles were often out of the plane of section and therefore not fully visible.

Figure 9 shows a top view of two squid chromatophores. Figure 9a is a yellow chromatophore layer that has one visible pigment sac. The surrounding chromatophores are located adjacent to the sinus. Knowledge of the stains used helped to understand what structures surround the chromatophore. The yellow/brown colors from the Weigerts hematoxylin + Orange G- target the cell nucleus and acidophilic structures like muscles and reflective elements (iridophores). Nuclei in the connective tissue as well as the radial muscles are clearly evident. Aniline blue targets connective tissue, mainly comprised of collagen and elastin. It is evident that the chromatophore radial muscles (yellow) extends from the pigment sac into the

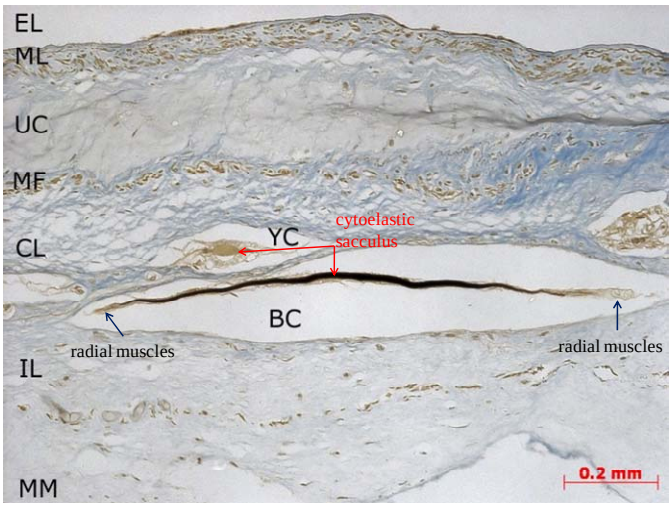

Figure 8: Thin (6µm) section of squid (*Loligo pealeii*) skin with outer epidermal layer (EL) and inner mantle muscle (MM) not shown. Dermis is composed of several layers: ML-muscle layer embedded in connective tissue, UC – small cells embedded in optically homogenous matrix, MF – Muscle fibers, CL – chromatophore layer, IL – iridophore layer. YC denotes a contracted yellow chromatophore. BC is an expanded brown chromatophore with radial muscles extending into the surrounding connective tissue.

connective tissue (blue) surrounding the chromatophores. The yellow (a) and red (b) chromatophores in Figure 9 display similar muscle arrangement and tethering.

4. DISCUSSION AND CONCLUSIONS

The bulge test results demonstrate that the chromatophore layer is a thin, highly elastic membrane capable of withstanding strains to an upper limit of 20% before failure. Within this layer, the chromatophores are situated in such a way that the pigment sacs are still intact after bulk failure of the skin layer. The tearing and deformation visualized for the chromatophore surface did not alter the pigment sac. The chromatophores themselves are isolated from the small strain damage incurred by the surface tissue.

The structural nature of the tissue surrounding the chromatophore is further validated with micro-DIC on live actuating tissue. Actuation of the chromatophore muscles and expansion of the pigment sac did not enact any noticeable change to the chromatophore surface layer. In addition, the actuation of one chromatophore did not influence the motion of surrounding chromatophores. This result suggests that chromatophores are mechanically decoupled from each other within the tissue.

Histologic sections of the squid chromatophores reveal that chromatophores are situated inside of a sinus cavity, with radial muscles extending into the connective tissue. The micro-DIC results from actuated tissue indicate the sinus structure protects the chromatophore. Chromatophore expansion occurs within the sinus, and the size of the sinus chamber appears to stay fixed even with chromatophore relaxation.

Finally, these results show that chromatophore networks are well designed to absorb small deformations and tensile damage without causing catastrophic damage or loss of function. These results demonstrate that it may be possible to design flexible materials with similar properties.

ACKNOWLEDGEMENTS

The authors thank Lydia Mathger, Eric Forsythe, Keran Lu, and Sanchao Liu for constructive discussions. This research was supported in part by an appointment to the Postgraduate Research Participation Program at the U.S. Army Research Laboratory administered by Oak Ridge Institute for Science and Education through an interagency agreement between the U.S. Department of Energy and USARL.

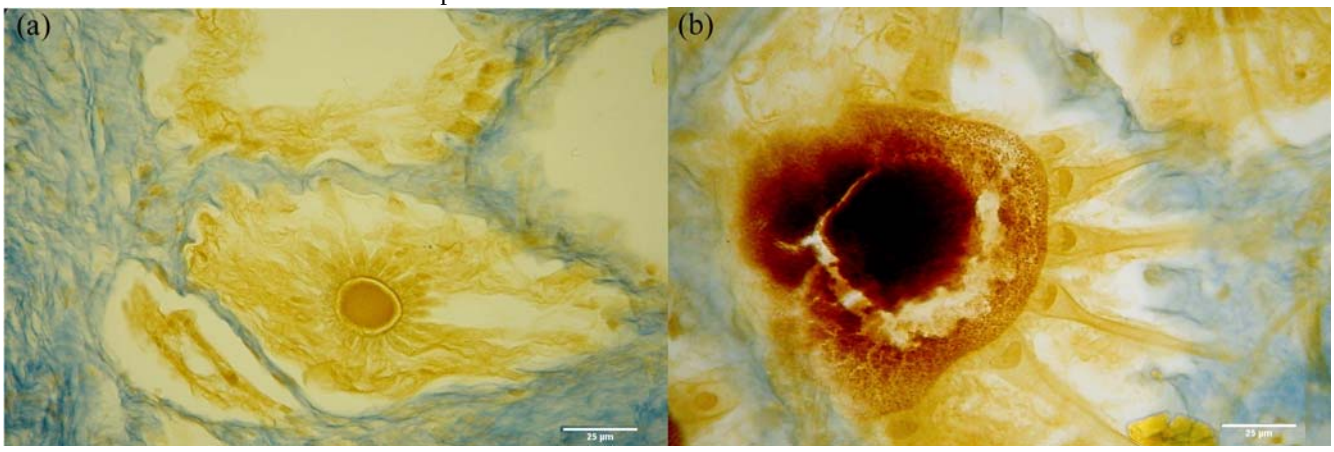

Figure 9: Micrographs of fixed (a) yellow and (b) red chromatophores stained using Weigert's Iron Hematoxylin and counterstained with solution II of Mallory's triple connective stain.

5. REFERENCES

Boyce, B. L.; J. M., Grazier; R. E., Jones; T. D., Nguyen, 2008: Full-field deformation of bovine cornea under constrained inflation conditions. *Biomaterials*, **29**, 3896-3904

Cloney, R. A., and E. Florey, 1968: Ultrastructure of cephalopod chromatophores. *Zeit. Zell.*, **89**, 250-280

Cloney, R. A., and S. L., Brocco, 1968: Chromatophore organs, reflector cells, iridocytes and leucophores in cephalopods. *American Zoologist*, **23**, 581-592

Dick, J. C., 1951: The tension and resistance to stretching of human skin and other membranes, with results from a series of normal and oedematous cases. *J. Physiol.*, **112**, 102-113

Elsheikh, A., and K. Anderson, 2005: Comparative study of corneal strip extensometry and inflation tests. *J. R. Soc. Interface*, **2**, 177-185

Florey, E., 1966: Nervous control and spontaneous activity of the chromatophores of a cephalopod. *Comp. Biochem. and Phys.*, **18**, 305-324

Florey, E., 1969: Ultrastructure and function of cephalopod chromatophore organs. *American Zoologist*, **9**, 429-442

Fung, Y. C., 1993: *Biomechanics***:** Mechanical Properties of Living Tissues. 2nd ed. Springer.

Gosline, J.; M. Lillie; E. Carrington; P. Guerette; C. Ortlepp; K. Savage, 2002: Elastic proteins: biological roles and mechanical properties. *Phil. Trans. R. Soc. Lond. B*, **357**, 121-132

Hanlon, R. T., 1982: The functional organization of chromatophores and iridescent cells in the body patterning of *Loligo plei*. *Malacologia*, **23**, 89-119

Hanlon, R. T., 2007: Cephalopod dynamic camouflage. *Current Biology*, **17**, R400-R404

Hanlon, R. T., and J. B., Messenger, 1988: Adaptive coloration in young cuttlefish (*Sepia officinalis* L.): the morphology and development of body patterns and their relation to behaviour. *Phil. Trans. R. Soc. B*, **320**, 437-487

Hanlon, R. T., and J. B., Messenger, 1996: *Cephalopod Behaviour*. Cambridge University Press.

Hanlon, R. T.; K. M., Cooper; B. U., Budelmann; T. C., Pappas, 1990: Physiological color-change in squid iridophores. I. Behavior, morphology and pharmacology in *Lolliguncula brevis*. *Cell Tissue Res.*, **259**, 3-14

Humason, G. L., 1967: *Animal Tissue Techniques*. W.H. Freeman and Sons.

Mallory, F. B., 1944: *Pathological Technique*. W.B. Saunders and Company.

Mathger, L. M., and R. T., Hanlon, 2007: Malleable skin coloration in cephalopods: selective reflectance, transmission and absorbance of light by chromatophores and iridophores. *Cell Tissue Res.*, **329**, 179-186

Messenger, J. B., 2001: Cephalopod chromatophores: neurobiology and natural history. *Biol. Rev.*, **76**, 473-528

Messenger, J. B.; C. J. Cornwell; C. M. Reed, 1997: L-Glutamate and serotonin are endogenous in squid chromatophore nerves. *J. Exp. Biol.*, **200**, 3043-3054

Mirow, S., 1972: Skin color in the squids *Loligo pealii* and *Loligo opalescens*. I. Chromatophores. *Zeit. Zell.*, **125**, 143-175

Packard, A., 1995: Organization of cephalopod chromatophore systems: a neuromuscular image-generator. *Cephalopod Neurobiology*. Abbott, N. J., Williamson, R.; Maddock, L., Eds., Oxford University Press, p. 331-368.

Reed, C. M., 1995a: The ultrastructure and innervation of muscles controlling chromatophore expansion in the squid, *Loligo vulgaris*. *Cell Tissus Res.*, **282**, 503-512

Reed, C. M., 1995b: Dye coupling in the muscles controlling squid chromatophore expansion. *J. Exp. Biol.*, **198**, 2631-2634

Romeis, B., 1948: *Mikrosckopischen Technick*. Leibniz Verlag.

Small, M. K., and W. D., Nix, 1992: Analysis of the accuracy of the bulge test in determining the mechanical properties of thin films. *J. Mater. Res.*, **7**, 1553-1563

Steedman, H. F., 1947: Esterwax; a new embedding medium. *Quart. J. Microsc. Sci.*, **88**, 123-133

Stuart-Fox, D.; A. Moussalli; M. J., Whiting, 2008: Predator-specific camouflage in chameleons. *Biol. Lett.*, **4**, 326-329

Sutton, M. A.; X. Ke; S. M. Lessner; M. Goldbach; M. Yost; F. Zhao; H. W. Schreier, 2008: Strain field measurements on mouse carotid arteries using microscopic three-dimensional digital image correlation. *J. Biomed. Mater. Res. Part A*, **84**, 178-190

Sweeney, A. M.; D. L., Des Marais; Y.-E. A., Ban; S. Johnsen, 2007: Evolution of graded refractive index in squid lenses. *J. R. Soc. Interface*, **4**, 685-698

Xiang, Y.; X. Chen; J. J., Vlassak, 2005: Plane-strain bulge test for thin films. *J. Mater. Res.*, **20**, 2360-2370

Young, W. C., and R. G., Budynas, 2002: *Roark's formulas for stress and strain*. 7th. ed. McGraw-Hill Companies, Inc, 554 p.

NO. OF
COPIES ORGANIZATION

1 ADMNSTR
DEFNS TECHL INFO CTR
ATTN DTIC OCP
8725 JOHN J KINGMAN RD STE 0944
FT BELVOIR VA 22060-6218

3 MARINE RESOURCES CENTER
MARINE BIOLOGICAL LABORATORY
ATTN R HANLON (3 HCS)
7 MBL ST
WOODS HOLE MA 02543

6 US ARMY RSRCH LAB
ATTN RDRL WMM A K KIRKWOOD (6 HCS)
BLDG 4600
ABERDEEN PROVING GROUND MD 21005

1 US ARMY RSRCH LAB
ATTN RDRL CIM G T LANDFRIED
BLDG 4600
ABERDEEN PROVING GROUND MD 21005-5066

3 US ARMY RSRCH LAB
ATTN IMNE ALC HRR MAIL & RECORDS MGMT
ATTN RDRL CIM L TECHL LIB
ATTN RDRL CIM P TECHL PUB
ADELPHI MD 20783-1197

INTENTIONALLY LEFT BLANK.